Implementation of Various Approaches for Iris Image Normalization

Namrata P. Joshi, Roopal K. Lamba, Devang U. Shah, Bhargav V. Ghadia

Abstract-- **A biometric system provides automatic identification of an individual, based on a unique feature or characteristic possessed by the individual. Iris recognition is regarded as the most reliable and accurate biometric identification system available. Here, the segmented iris region is processed to allow comparisons with existing database (Normalization and Enhancement). The normalization process will produce iris regions, which have the same constant dimensions, so that two photographs of the same iris under different conditions will have characteristic features at the same spatial location.**

To convert iris into dimensionally compatible form, normalization technique was studied and various approaches of normalization are implemented. When needed, these approaches have been modified to achieve better performance. This electronic document represents implementation of various techniques for validation of this work.

Index Terms—**Analysis band based normalization, Basic rubber sheet model, Dimension reduction approach, Rubber sheet model of lower half of iris, Sector based normalization.**

I. INTRODUCTION

A biometric system provides automatic recognition of an individual based on some sort of unique feature or characteristic possessed by the individual.

A good biometric is characterized by use of a feature that is; highly unique – so that the chance of any two people having the same characteristic will be minimal, stable – so that the feature does not change over time, and be easily captured – in order to provide convenience to the user, and prevent misrepresentation of the feature. The human iris is best suitable for this application.

Iris recognition is a method of biometric authentication that uses pattern-recognition techniques based on high-resolution images of the irises of an individual's eyes. Here, person's eye image is captured (Data Acquisition), the iris region is separated from the rest of the eye image (Segmentation), this iris region is processed to allow comparisons with existing database (Normalization and Enhancement) and finally the specific features from the resulting image is extracted to compare with the database (Feature Extraction).

Robust representations for pattern recognition must be invariant to changes in the size, position, and orientation of the patterns. In the case of iris recognition, this means we must create a representation/template that is invariant to the optical size of the iris in the image (which depends upon the distance to the eye, and the camera optical magnification factor); the size of the pupil within the iris (which introduces a nonaffine pattern deformation); the location of the iris within the image; and the iris orientation, which depends upon head tilt, torsional eye rotation within its socket (cyclovergence), and camera angles, compounded with imaging through pan/tilt eye-finding mirrors that introduce additional image rotation factors as a function of eye position, camera position, and mirror angles. For this, segmented iris region should be converted into dimensionally consistent representation of the iris region.

This paper presents various iris normalization strategies studied and implemented to remove dimensional inconsistencies in order to produce normalized iris template. Some modifications are proposed for the existing techniques to achieve optimized results.

The main objective of this paper is to implement iris image normalization techniques and find the best suitable approach by comparing them.

II. APPROACHES FOR IRIS NORMALIZATION

The approaches for normalization discussed in this paper are

1. Basic rubber sheet model
2. Rubber sheet model of lower half of iris
3. Sector based normalization
4. Analysis band based normalization
5. Dimension reduction approach

1. Basic Rubber Sheet Model

For normalization of iris regions a technique based on Daugman's rubber sheet model [1] [2] is employed.

The center of the pupil was considered as the reference point, and radial vectors pass through the iris region.

A number of data points are selected along each radial line and this is defined as the radial resolution. The number of radial lines going around the iris region is defined as the angular resolution. Since the pupil can be non-concentric to the iris, a remapping formula is needed to rescale points depending on the angle around the circle.

The remapping formula first gives the radius of the iris region 'doughnut' as a function of the angle θ.

A constant number of points are chosen along each radial line, so that a constant number of radial data points are taken, irrespective of how narrow or wide the radius is at a particular angle. The normalized pattern was created by backtracking to find the Cartesian coordinates of data points from the radial and angular position in the normalized pattern, as shown in Fig. 1.

978-1-4577-2168-7/11/$26.00 ©2011 IEEE

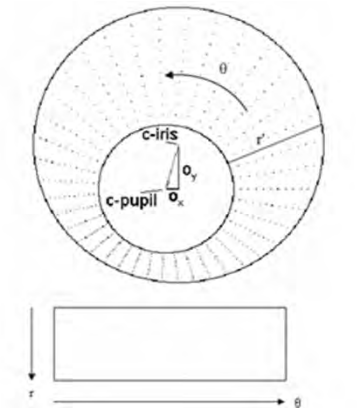

Fig. 1. Daugman's Rubber Sheet model

From the 'doughnut' iris region, normalization produces a 2D array with horizontal dimensions of angular resolution and vertical dimensions of radial resolution. This is done by interpolation techniques, viz. Bilinear interpolation and Bicubic interpolation.

2. Rubber Sheet Model of Lower Half of Iris

In normal gaze, the iris is partially covered with eyelids. This can lead to false recognition result. To avoid the prominent occlusion due to upper eyelid this technique was implemented. The resulting Rubber Sheet model will be made from only the lower half of the iris [3].

3. Sector Based Normalization

There exists traditional method for iris normalization that transforms the detected annular ring into a rectangular block. However, the normalized iris image is occluded by eyelashes and eyelids. In a normal gaze the edge of the upper eyelid intersects the sclera and approximately half of the upper iris circle whereas lower eyelid covers one-fourth of the lower iris circle. However the left and right regions are independent of such occlusions. Depending upon their degree of motion upper eyelids add more noise to the transformed strip as compared to lower eyelid.

The sector based normalization [4] helps to minimize such occlusions. In this approach non-occluded region is considered by taking variable size of sectors during transformation from Cartesian to polar domain. For certain range of angular values the radial dimension along left and right sector are taken completely because no occlusion occurs here. However for the upper and lower region only partial values are taken in the sector.

4. Analysis Band Based Normalization

As discussed previously, the segmented iris has frequent partial occlusion by upper and lower eyelids. Also the specular reflection from cornea obscures the part of lower iris portion. These areas should be excluded from analysis and encoding. For this, the portion of the iris to be analyzed is mapped and subdivided into eight analysis bands. These analysis bands [5] are defined in the normalized rubber sheet model.

5. Dimension Reduction Approach

This approach [6] attempts to reduce the dimensionality of the problem while focusing only on parts of the scene that effectively identify the individual. Also, the mapping of iris is restricted to the areas known to have less influence of eyelashes and eyelids, i.e. the sides of the iris.

Here two portions having the size equal to that of pupil size from the left and right side of the iris are considered. After performing normalization operation, these two portions are merged. The resulting image will be having minimal or no influence of noises.

III. CALCULATIONS

1. Daugman's Basic Rubber Sheet Model

The remapping formula needed to rescale points depending on the angle around the circle is given by

$$r' = (\alpha)^{1/2}\beta \pm (\alpha\beta^2 - \alpha - r_I^2)^{1/2} \quad (1)$$

With

$$\alpha = O_x^2 + O_y^2,\ \beta = \cos(\pi - \Phi - \theta)$$

Where

$$\Phi = \arctan(O_x / O_y) \text{ and } \theta \rightarrow [0, 2\pi]$$

Here displacement of the center of the pupil relative to the center of the iris is given by O_x and O_y. r' is the distance between the edge of the pupil and edge of the iris at an angle, θ around the region, and r_I is the radius of the iris [4].

Formula for anticlockwise unwrapping of iris is given by

$$x_0 = x_p + (r \times \cos\theta),\ y_0 = y_p + (r \times \sin\theta) \quad (2)$$

Where

$$x_p, y_p = \text{pupil center coordinates}$$

$$\theta = (2\pi / \text{angular resolution}) \text{ where } \theta \rightarrow [0, 2\pi]$$

2. Rubber Sheet Model of Lower Half of iris

Here, the implementation steps are same as those of Basic Rubber Sheet Model. But the range of θ is made $[\pi, 2\pi]$ instead of $[0,2\pi]$ to eliminate the upper half portion of iris. Thus, remapping formula will be same except the range of θ.

3. Sector Based Normalization

The normalization procedure implementation is same as that of Basic Rubber Sheet Model. The non-concentricity of pupil within iris is also taken care of. But here, the value of r and θ varies for different sectors depending upon the occlusion. Some modifications in sector dimensions have been done to improve results.

The sectors are resized to make eyelid removal more efficient. Sector 1 now has θ ranges from [315° 30°] and r ranges from [0 1]. For sector 2, θ ranges from [31° 165°] and r ranges from [0 0.5]. For sector 3, θ ranges from [166° 235°] and r ranges from [0 1]. For sector 4, θ ranges from [236° 314°] and r ranges from [0 0.75], as shown in Fig. 2.

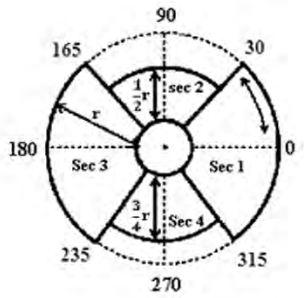

Fig. 2. Sector dimensions

Sector 2 and sector 4 are padded with NaN and then all the sectors are concatenated to make a normalized iris image.

4. Analysis Band Based Normalization

Four additional special features of the analysis bands are needed to compensate for the departure of many iris images from the ideal, annular stereotype. First, since the pupil itself often has an irregular boundary, the innermost analysis band starts with a radius of about 1.1 times the pupil's average radius in order to ensure exclusion of pupil entirely. Similarly, since the transition from iris to sclera may likewise be irregular and non-circular, the outermost analysis band extends radially only to about 80% of the distance to the outer boundary of the iris (as measured to the right and left, with cosinusoidal weighing in intermediate angles). Third, provision must be made for the occlusion of the upper and lower portions of the iris by the eyelid, and fourth, for a specular reflection that may cover part of the iris if an oblique source of illumination is used (typically from below).

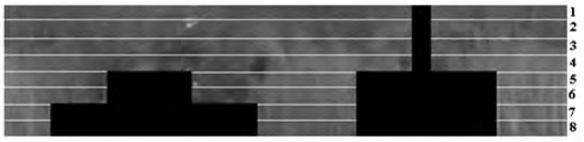

Fig. 3. Analysis Band Based Normalization

5. Dimension Reduction approach

The output of segmented iris image is center coordinates and radius of iris and pupil respectively. From these data, iris endpoints and height of pupil are retrieved. The space s between the rows of resulting normalized image is calculated. Also, the index of first target row at the top of pupil is also calculated. The width of rows of the iris portion of interest is calculated for both sides of pupil. For all rows, starting at the top of the pupil, ending at the bottom of the pupil and spaced by space s, the location of the pixel nearest to the pupil is found out by using equation of circle. This is again done for both the sides of pupil. The equations for the nearest pixels situated on the right and left side of pupil are given as,

$$right_{pixel} = [r_x^2 - (row - c_y)^2]^{1/2} + c_x \quad (3)$$

$$left_{pixel} = -[r_x^2 - (row - c_y)^2]^{1/2} + c_x \quad (4)$$

Where c_x, c_y = pupil center, r_x = horizontal radius of pupil, row = row width

For every row, the pixels lying between the nearest pixel and iris endpoint pixel of the respective sides are mapped in to another empty matrix and this is done for each side. An average mask of 3 × 3 pixels is used to calculate pixel intensity. Both the matrices are then merged side by side to form final normalized iris image.

IV. RESULTS

These approaches are implemented upon 130 images of CASIA database [7], 300 images of UBIRIS (800 × 600) database and 340 images of UBIRIS (200 × 150) database [8]. MATLAB (R2009b) is used as the development tool. The computer system used has Intel Pentium 4 CPU, 3.06 GHz, 0.99 GB RAM.

TABLE I
RESULTS FOR BASIC RUBBER SHEET MODEL

Database	Resulting images without iris occlusion	Resulting images with iris occlusion	Image quality	Execution time (Bilinear) (seconds)	Execution time (Bicubic) (seconds)
CASIA	21%	79%	Very good	0.15	0.18
UBIRIS (800 × 600)	35%	65%	Good	0.20	0.22
UBIRIS (200 × 150)	40%	60%	Fair	0.3	0.29

TABLE II
RESULTS FOR RUBBER SHEET MODEL OF LOWER HALF OF IRIS

Database	Resulting images without iris occlusion	Resulting images with iris occlusion	Image quality	Execution time (seconds)
CASIA	70%	30%	Very good	0.15
UBIRIS (800 × 600)	85%	15%	Good	0.20
UBIRIS (200 × 150)	87%	13%	Fair	0.16

TABLE III
RESULTS FOR SECTOR BASED NORMALIZATION

Database	Resulting images without iris occlusion	Resulting images with iris occlusion	Image quality	Execution time (seconds)
CASIA	75%	25%	Very good	0.27
UBIRIS (800 × 600)	90%	10%	Good	0.20
UBIRIS (200 × 150)	94%	6%	Fair	0.16

TABLE IV
RESULTS FOR ANALYSIS BAND BASED NORMALIZATION

Database	Resulting images without iris occlusion	Resulting images with iris occlusion	Image quality	Execution time (seconds)
CASIA	83%	17%	Very good	0.3
UBIRIS (800 × 600)	89%	11%	Good	0.21
UBIRIS (200 × 150)	91%	9%	Fair	0.17

TABLE V
RESULTS FOR DIMENSION REDUCTION APPROACH

Database	Resulting images without iris occlusion	Resulting images with iris occlusion	Image quality	Execution time (seconds)
CASIA	92%	8%	Very good	1.6
UBIRIS (800 × 600)	98%	2%	Good	1.6
UBIRIS (200 × 150)	98%	2%	Fair	1.6

The resulting normalization templates for various normalization approaches are shown below.

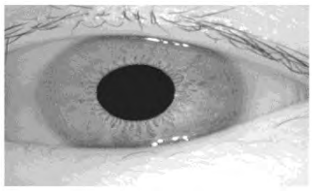

Fig. 4. Original eye image

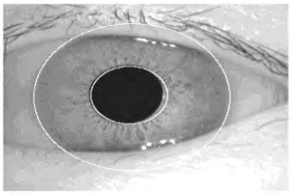

Fig. 5. Segmented eye image

Fig. 6. Basic Rubber sheet model of iris

Fig. 7. Rubber sheet model of lower half of iris

Fig. 8. Sector based normalization

Fig. 9. Analysis band based normalization

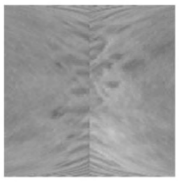

Fig. 10. Dimension reduction approach

V. CONCLUSION

These approaches are implemented upon 130 images of CASIA database, 300 images of UBIRIS (800 × 600) database and 300 images of UBIRIS (200 × 150) database. For performance evaluation of the algorithms, MATLAB (R2009b) is used as the development tool. The computer system used has Intel Pentium 4 CPU, 3.06 GHz, 0.99 GB RAM. The evaluation of implementation techniques is done by visual inspection of results and execution time.

By observing the normalized image it is seen that basic Rubber sheet model technique is easier to implement. Although scaling of pupil and iris radius have been done to eliminate its residual effect, the resulting images are highly influenced by noises like eyelid occlusion, eyelashes occlusion and reflection. Also, image quality is not good enough. Moreover, the effects of interpolation techniques cannot be seen by visual detection but can be seen at the feature extraction and matching stage.

The Rubber sheet model of lower half of iris eliminates the influence of upper eyelid, but if lower eyelid occlusion is present, it is needed to be masked. Also, there is higher iris information loss.

The sector based normalization causes less information loss as here the areas having maximum possibilities of eyelid occurrence are masked. But as the exact eyelid location is not detected here, some information loss or sometimes, partial eyelid masking results. Same is in the case of Analysis band based normalization.

In dimension reduction approach, there is data loss, but here the essential information is preserved and no separate masking or detection of noise is necessary. The execution time is slightly higher, but its reduced dimension with distinct information speeds up further process.

VI. REFERENCES

[1] J. Daugman, 'How iris recognition works', Proceedings of 2002 International Conference on Image Processing, Vol. 1, 2002.

[2] Libor Masek., 'Recognition of human iris patterns for biometric identification', Technical Report, School of Computer Science and Software Engineering, University of Western Australia, 2003.

[3] K. Miyazawa, K. Ito, T. Aoki, K. Kobayashi, H. Nakajima, "An Effective Approach for Iris Recognition Using Phase-Based Image Matching", IEEE Transactions On Pattern Analysis And Machine

Intelligence, Vol. 30, No. 10, pp. 1741-1756, October 2008.

[4] Mehrotra, H.; Badrinath, G.S.; Majhi, B.; Gupta, P.;, "An Efficient Iris Recognition Using Local Feature Descriptor", Image Processing (ICIP), 16th IEEE International Conference on Digital Object Identifier, pp. 1957-1960, 2009.

[5] J. Daugman, 'Biometric Personal Identification System Based on Iris Analysis', United States Patent, March 1994.

[6] P. Merloti, "Experiments on Human Iris Recognition Using Error Back Propagation Artificial Neural Network", Final project, San Diego State University, April 2004.

[7] Chinese academy of Sciences, I.O.A, 'CASIA iris Image Database', Available at: http//www.sinobiometrics.com/resources.htm

[8] Proenc, H. and Alexandre, L. A., 'Ubiris Iris Image Database at: iris.di.ubi.pt', 2004.

[9] Gonzalez, Woods, 'Digital Image Processing', second edition, Prentice Hall, 2001.